Planta (2012) 236:1639–1652
DOI 10.1007/s00425-012-1710-2

ORIGINAL ARTICLE

Cold acclimation and *BnCBF17*-over-expression enhance photosynthetic performance and energy conversion efficiency during long-term growth of *Brassica napus* under elevated CO_2 conditions

Keshav Dahal · Winona Gadapati · Leonid V. Savitch · Jas Singh · Norman P. A. Hüner

Received: 4 March 2012 / Accepted: 6 July 2012 / Published online: 31 July 2012

Abstract The effects of cold acclimation and long-term elevated CO_2 on photosynthetic performance of wild-type (WT) and *BnCBF17*-over-expressing line of *Brassica napus* cv. Westar (*BnCBF17*-OE) grown at either 20/16 °C (non-acclimated) or 5/5 °C (cold acclimated) and at either ambient (380 μmol C mol^{-1}) or elevated (700 μmol C mol^{-1}) CO_2 were studied. Compared with non-acclimated WT, the *BnCBF17*-OE grown at 20 °C mimicked the effects of cold acclimation on WT *B. napus* with respect to compact dwarf phenotype and increased rates of light-saturated CO_2 assimilation and photosynthetic electron transport. This was associated with enhanced energy conversion efficiency into biomass as assessed by decreased excitation pressure coupled to decreased dependence on non-photochemical energy dissipation for a given irradiance. Growth at elevated CO_2 decreased the light and CO_2-saturated rates of photosynthesis by 30 % for non-acclimated WT relative to growth at ambient CO_2. This was associated with inhibition in electron transport rates (20 %), decrease in amount of rbcL (35 %) and cytosolic FBPase (70 %) and increased excitation pressure and non-photochemical quenching in elevated versus ambient CO_2-grown non-acclimated WT. In contrast, light and CO_2-saturated rates of photosynthesis, electron transport, excitation pressure, non-photochemical quenching and levels of rbcL, cytosolic FBPase and Lhcb1 were insensitive to growth under elevated CO_2 in *BnCBF17*-OE and cold-acclimated WT. Thus, *BnCBF17*-over-expression and cold acclimation maintain enhanced energy conversion efficiency and reduced sensitivity to feedback-limited photosynthesis during long-term growth of *B. napus* under elevated CO_2. Our results indicated that CBFs transcription factors regulate not only freezing tolerance but also has major whole plant effects.

Keywords *BnCBF17*-over-expression · *Brassica* · Cold acclimation · Energy conversion efficiency · Long-term elevated CO_2 · Photosynthesis

Abbreviations

CA	Cold acclimated
NA	Non-acclimated
WT	Wild-type *Brassica napus*
BnCBF17-OE	*B. napus* line over-expressing cold-binding transcription factor BnCBF17
A_{sat}	Light-saturated rates of CO_2 assimilation
R_{dark}	Dark respiration rates
PPFD	Photosynthetic photon flux density
C_i	Internal leaf CO_2 concentrations

Electronic supplementary material The online version of this article (doi:10.1007/s00425-012-1710-2) contains supplementary material, which is available to authorized users.

K. Dahal (✉) · W. Gadapati · N. P. A. Hüner (✉)
Department of Biology, The Biotron Centre for Experimental Climate Change Research, The University of Western Ontario, London, ON N6A 5B7, Canada
e-mail: kdahal@uwo.ca

W. Gadapati
e-mail: wgadapa2@uwo.ca

N. P. A. Hüner
e-mail: nhuner@uwo.ca

L. V. Savitch · J. Singh
Eastern Cereal and Oilseed Research Centre, Agriculture and Agri-Food Canada, Ottawa, ON K1A OC6, Canada
e-mail: leonid.savitch@agr.gc.ca

J. Singh
e-mail: jas.singh@agr.gc.ca

ETR	Maximum rate of photosynthetic electron transport estimated from room temperature Chl-a fluorescence induction
J_{max}	Maximum rate of photosynthetic electron transport calculated from CO_2 gas exchange
EP	Excitation pressure measured as 1-qP, the proportion of closed PSII reaction centres
NPQ	Non-photochemical quenching, an estimate of the capacity to dissipate energy as heat
Q	Apparent maximum quantum efficiency for CO_2 assimilation
CE	Carboxylation efficiency
V_{cmax}	Maximum capacity of Rubisco carboxylation
rbcL	Large subunit of Rubisco
cFBPase	Cytosolic fructose-1,6-bisphosphatase
SPS	Sucrose phosphate synthase
Lhcb1	The major PSII light harvesting protein
g_s	Stomatal conductance
WUE	Instantaneous leaf level water use efficiency

Introduction

The effects of cold acclimation on plant morphology, physiology and biochemistry have been widely studied in cold-tolerant wheat, rye and barley as well as spinach, *Arabidopsis thaliana* and *Brassica napus* (Krause 1988; Hüner et al. 1993, 1998; Adams et al. 2002; Stitt and Hurry 2002; Öquist and Hüner 2003; Savitch et al. 2005; Ensminger et al. 2006). Cold acclimation of winter rye, winter wheat (Hüner et al. 1981, 1985; Dahal et al. 2012a), spinach (Boese and Hüner 1990) as well as *Arabidopsis thaliana* (Strand et al. 1999; Gorsuch et al. 2010a, b) and *B. napus* (Savitch et al. 2005; Dahal et al. 2012a) exhibit altered plant phenotype and growth habit. Growth and development of cold-tolerant plants at low temperature generally results in a compact, dwarf growth habit with leaves that exhibit increased thickness relative to NA controls (Hüner et al. 1981, 1985; Dahal et al. 2012a). The increased leaf thickness associated with the cold-acclimated state can be accounted for by either increases in leaf mesophyll cell size (Hüner et al. 1981; Gorsuch et al. 2010a) and/or increases in the number of palisade layers (Boese and Hüner 1990; Dahal et al. 2012a).

Cold acclimation of cold-tolerant species generally results in enhanced light-saturated rates of photosynthesis, A_{sat}, at measuring temperatures of either 5 or 20 °C (Dahal et al. 2012a). It has been suggested that the cold acclimation-induced increase in A_{sat} of cold-tolerant species such as wheat, rye, *A. thaliana* and *B. napus*, is correlated with a stimulation of carbon metabolism as a result of the enhanced activities of key regulatory photosynthetic enzymes such as Rubisco, cFBPase and SPS in response to low growth temperatures (Hurry et al. 2000; Stitt and Hurry 2002; Savitch et al. 2005). Our recent study (Dahal et al. 2012a) has revealed that the increased A_{sat} of CA winter wheat and winter rye especially when measured on a leaf area basis can, by and large, be accounted for by the increased specific leaf weight in response to growth at low temperature. There is a strong, positive correlation between the cold acclimation-induced increase in A_{sat} and the development of freezing tolerance as well as an increased resistance to low temperature-induced photoinhibition in winter rye and winter wheat (Hüner et al. 1993; Öquist et al. 1993; Sarhan et al. 1997; Pocock et al. 2001), spinach (Krause 1988; Somersalo and Krause 1989; Guy 1990; Boese and Hüner 1992; Gray et al. 1997), *A. thaliana* (Savitch et al. 2001) and *B. napus* (Savitch et al. 2005). The increased resistance to photoinhibition and decreased temperature sensitivity of photosynthetic performance associated with cold acclimation are governed by changes at the cellular and biochemical levels rather than at the level of leaf anatomy and morphology and are characterized by an increased quantum requirement to close PSII reaction centers (Dahal et al. 2012a).

What governs this complex, integrated phenomenon in cold-tolerant plant species? It has been suggested that CBFs/DREBs (cold-binding transcription factors/dehydration responsive element binding factors) appear to control the phenotypic plasticity, biochemical changes and photosynthetic performance in cold-tolerant species (Liu et al. 1998; Kasuga et al. 1999; Gilmour et al. 2000, 2004; Savitch et al. 2005). For instance, even at a growth temperature of 20 °C, the over-expression of *BnCBF17* (Savitch et al. 2005) and *AtCBF3* (Gilmour et al. 2000, 2004) mimic multiple phenotypic, physiological and biochemical changes as observed upon cold acclimation of their wild type (WT) counterparts. Similar results have been reported for over-expression of *AtCBF1* in potato (Pino et al. 2008), tobacco (Yang et al. 2010), tomato *CBF1* in transgenic *Arabidopsis* (Zhang et al. 2004) and *EguCBF1* in *Eucalyptus* (Navarro et al. 2011). Our recent study has revealed that over-expression of *BnCBF17* in *B. napus* grown at 20 °C mimics the effects of cold acclimation of winter rye and winter wheat with respect to increased SLW, increased leaf thickness, improved WUE, enhanced light-saturated rates of CO_2 assimilation and photosynthetic electron transport coupled with a decrease in the low temperature sensitivity of these processes (Dahal et al. 2012a). Thus,

over-expression of *B. napus* with a single transcription factor, *BnCBF17*, appears to cause the conversion of non-acclimated WT to a cold acclimated state without exposure to low growth temperature. CBFs/DREBs are a family of transcriptional activators required to induce the expression of cold-regulated genes (*COR*) that enhance plant freezing tolerance (Liu et al. 1998; Kasuga et al. 1999; Gilmour et al. 2000; van Buskirk and Thomashow 2006; Chinnusamy et al. 2007; Badawi et al. 2008). In addition to enhanced freezing tolerance (Savitch et al. 2005), over-expression of *BnCBF17* has much broader effects on plant phenotype, leaf anatomy, photosynthetic performance, water use efficiency and dry matter accumulation typically associated with cold acclimation of winter cereals and *B. napus* (Dahal et al. 2012a). Thus, CBFs/DREBs appear to be critical factors that govern plant phenotypic plasticity during cold acclimation.

An immediate increase in the rates of net CO_2 assimilation has been observed following short-term shift of C_3 plants from ambient to elevated CO_2 (Cheng et al. 1998; Long et al. 2004; Ainsworth and Rogers 2007; Dahal et al. 2012b). This CO_2 stimulation of photosynthesis in C_3 plants is attributed to two factors. First, at current ambient CO_2 concentrations, Rubisco is CO_2-limited as the K_m (CO_2) for Rubisco is close to the current atmospheric CO_2 concentration (Long et al. 2004; Tcherkez et al. 2006). Thus, an increased CO_2 substrate availability for Rubisco immediately enhances carboxylation velocity. Second, elevated CO_2 competitively suppresses photorespiration because CO_2 is a competitive inhibitor of the oxygenation of RuBP by Rubisco (Long et al. 2004).

However, long-term growth and development of C_3 plants at high CO_2 concentration may lead to an end product inhibition of photosynthetic capacity due to accumulation of non-structural carbohydrates in the cytosol (Stitt and Quick 1989; Foyer 1990). This feedback inhibition of photosynthesis in response to growth at elevated CO_2 may result from the chloroplastic P_i-limitation in the short-term and down-regulation of the expression and activities of key regulatory photosynthetic enzymes in the long-term (Harley and Sharkey 1991; Drake et al. 1997; Moore et al. 1999).

Previous studies have shown that over-expression of *BnCBF17* in *B. napus* mimics the effects of cold acclimation with respect to enhanced photosynthetic performance at ambient CO_2 (Savitch et al. 2005; Dahal et al. 2012a). The objective of this study is to assess whether the enhanced photosynthetic performance observed for *BnCBF17*-OE as well as cold acclimated WT relative to non-acclimated WT *B. napus* at ambient CO_2 (380 μmol C mol^{-1}) is maintained upon long-term growth and development at elevated CO_2 (700 μmol C mol^{-1}). Since cold acclimated WT *B. napus* exhibits enhanced sink capacity and increased activities of major photosynthetic enzymes (Savitch et al. 2005; Dahal et al. 2012a), we hypothesize first that, cold acclimation-induced increase in photosynthetic performance of *B. napus* at ambient CO_2 is maintained under long-term growth and development at elevated CO_2. Second, we hypothesized that the *BnCBF17*-OE grown at 20 °C should respond similarly to growth and development under elevated CO_2 as does cold acclimated WT *B. napus*.

Materials and methods

Plant growth

Brassica napus cv. Westar (wild type) and the *B. napus* *BnCBF17*-over-expressing transgenic line (*BnCBF17*-OE) were used in all experiments. Seeds of WT and *BnCBF17*-OE were obtained from Agriculture and Agri-Food Canada, Ottawa, Canada. The *BnCBF17*-over-expressing line was generated as described in detail by Savitch et al. (2005). Seeds of WT and *BnCBF17*-OE were grown in controlled environmental growth chambers (Model: GCW15 chamber, Environmental Growth Chambers, Chargin Falls, OH, USA) at either ambient CO_2 (380 ± 10 μmol C mol^{-1}) or elevated CO_2 (700 ± 25 μmol C mol^{-1}) with a PPFD of 250 ± 20 μmol photons m^{-2} s^{-1}, 50–60 % relative humidity and a 16 h photoperiod. The WT plants were grown at day/night temperature regimes of either 20/16 °C non-acclimated (NA) or 5/5 °C cold acclimated (CA) whereas the *BnCBF17*-over-expressing line was grown only at 20/16 °C from the seed germination. The light in the growth chambers were supplied with metal halide lamps (Philips Lighting Company, Somerset, NJ, USA) and high pressure sodium lucalox lamp (GE Lighting Inc., Cleveland, OH, USA). Each CO_2 growth chamber was equipped with a computer-controlled CO_2 infra-red gas analyzer (Model: WMA-4 CO_2 Analyzer, PP Systems International Inc., Amesbury, MA, USA) which monitored CO_2 concentrations continuously. In addition, the temperature, relative humidity, irradiance level and photoperiod in each chamber were computer-controlled and monitored continuously. The seedlings were grown in organic soil (Promix, Premier Horticulture, Quakertown, PA, USA) in 500 mL-sized plastic pots with one plant each and watered with all purpose fertilizer (Plant Prod 20–20–20, Sure-Gro IP Inc., Brantford, ON, Canada). The non-acclimated WT plants were grown for 3 weeks, the *BnCBF17*-OE for 4 weeks and the cold acclimated WT for 12 weeks from the seed germination. At these ages, the third leaves were fully expanded in non-acclimated WT, *BnCBF17*-OE and cold acclimated WT plants. Thus, all measurements of CO_2 gas exchange rates and Chl-a room temperature fluorescence and biochemical analyses were carried out on fully expanded third leaves of the 3-week-old

non-acclimated WT, 4-week-old *BnCBF17*-OE and 12-week-old cold acclimated WT *B. napus*.

The shoot and root fresh biomass were weighed, and the tissues were dried at 80 °C to constant weight for the determination of dry weight. Leaf blade area was measured by using a LI-COR portable area meter (LI–3000A, LI-COR Biosciences, Lincoln, NE, USA). Specific leaf weight (SLW) was calculated as leaf dry weight in g m^{-2} leaf blade area. The photosynthetic pigments, Chl-a and Chl-b, were quantified according to Arnon (1949).

In order to confirm that the pot size did not limit rooting volume and sink growth upon growth of plants at elevated CO_2, we carried out a pot size experiment for non-acclimated WT and *BnCBF17*-over-expressing *B. napus*. Plants were grown in various pot sizes of 0.3, 0.5, 1 and 1.5 L at elevated CO_2 (700 ± 30 µmol C mol^{-1}) and at growth conditions described above. Root and shoot biomass were harvested from 3-week-old non-acclimated WT and 4-week-old *BnCBF17*-OE, and the tissues were dried at 80 °C in order to get dry weight.

CO_2 gas exchange

Carbon dioxide gas exchange rates were measured on attached fully expanded third leaves at either 380 or 700 µmol C mol^{-1}. In addition, the CO_2 gas exchange rates for non-acclimated WT, cold-acclimated WT and *BnCBF17*-OE were made at the same measuring temperature of 20 °C irrespective of acclimation state. Our recent study has revealed that both cold acclimated WT and *BnCBF17*-OE are minimally sensitive to measuring temperatures between 5 to 25 °C for the rates of CO_2 gas exchange and electron transport (Dahal et al. 2012a). Carbon dioxide gas exchange rates were measured on attached fully expanded third leaves by using the LI-COR portable infrared CO_2 gas analyzer (LI-6400 XRT portable photosynthesis system, LI-COR Biosciences, Lincoln, NE, USA). Light response curves were measured using 12 irradiance values ranging from 0 to 1,300 µmol photons m^{-2} s^{-1} PPFD from high to low light intensity with 8 min of waiting time between each measurement. The apparent maximum quantum efficiency (Q) and the maximal photosynthetic capacity (A_{sat}) were determined as the maximum initial slope and the maximum light-saturated rates, respectively from light response curves. Carbon dioxide response curves were measured by supplying 11 different CO_2 values over the range of 50 to 1,200 µmol C mol^{-1} at a saturating irradiance of 1,300 µmol photons m^{-2} s^{-1} PPFD at 20 °C. Rubisco-limited carboxylation efficiency (CE) was calculated as the maximum initial slope and the CO_2-saturated photosynthesis as the plateau of the curves. The maximum Rubisco carboxylation capacity (V_{cmax}) and the maximum rates of electron transport (J_{max}) were calculated using the FCB photosynthesis model (Farquhar et al. 1980). Respiration rates (R_{dark}) were measured in the dark at either 380 or 700 µmol C mol^{-1} at the same measuring temperature of 20 °C irrespective of acclimation state. Measurements were made inside the CO_2 enriched chambers, to reduce diffusion errors through the leaf blade and chamber seals as suggested previously (Jahnke 2001; Jahnke and Krewitt 2002). In addition, stomatal conductance and leaf transpiration rates were measured simultaneously with CO_2 gas exchange measurements at growth CO_2 and 20 °C regardless of acclimation state. Instantaneous leaf level water use efficiency was calculated as µmol CO_2 fixed per mol of stomatal conductance (A/g_s). Stomatal density was estimated on both adaxial and abaxial leaf surface using a stage micrometer (1 mm^2) on a microscope (Leica ATC™ 2000, Buffalo, NY, USA). Stomata were counted at a magnification of 100×.

Room temperature Chl-a fluorescence

In vivo Chl-a fluorescence was measured to assess the effects of elevated CO_2 on maximum photochemical efficiency (F_v/F_m), maximum potential rates of photosynthetic electron transport (ETR), excitation pressure (EP), which estimates the relative reduction state of PSII reaction centers and non-photochemical quenching (NPQ), an estimate of the capacity to dissipate energy as heat. Chl-a fluorescence was measured simultaneously with CO_2 gas exchange on fully expanded third leaves using LI-COR portable photosynthesis system (LI-6400 XRT, LI-COR Biosciences). Light response curves of electron transport rates, excitation pressure and non-photochemical quenching of excess energy were measured at irradiance values ranging from 0 to 1,500 µmol PPFD photons, at 700 µmol C mol^{-1} and at a measuring temperature of 20 °C irrespective of growth CO_2 and irrespective of growth temperature. All measurements of Chl-a fluorescence were carried out using the standard fluorescence leaf chamber (2 cm^2). The leaves were dark-adapted for 20 min prior to fluorescence measurements. Minimum fluorescence (F_0) was measured by illuminating dark adapted leaves with a low irradiance measuring beam (PPFD < 1 µmol photons m^{-2} s^{-1}) from a light emitting diode. Maximal fluorescence (F_m) was determined by applying a flash of saturating light (PPFD > 5,000 µmol photons m^{-2} s^{-1}) for pulse duration of 0.8 s. Afterwards, an actinic light (PPFD 1,300 µmol photons m^{-2} s^{-1}) was applied. Superimposed on the actinic beam was a saturating light flash (PPFD > 5,000 µmol photons m^{-2} s^{-1}; 0.8 s) applied repetitively at 20 s intervals to determine maximal fluorescence in the light-adapted state (F'_m). Light adapted steady state fluorescence (F_s) was determined by measuring the level of fluorescence during steady-state photosynthesis.

Finally, minimal fluorescence (F_0') in the light-adapted leaf was measured by turning off the actinic light.

Determination of total leaf protein and immunodetection

The fully expanded third leaves were harvested, immediately frozen in liquid N_2 and stored at −80 °C. The leaf samples for the protein determination were prepared as described in detail by Dahal et al. (2012a). Total leaf protein content was quantified using the RC-DC protein assay kit (Bio-Rad, Hercules, CA, USA) according to the manufacturer's instructions. While quantifying the total leaf protein content, the addition of 1 μg of bovine serum albumin (Invitrogen, Carlsbad, CA, USA) in the extraction buffer was used as an internal standard.

The extracted proteins were electrophoretically separated using NuPAGE Novex 10 % (W/V) Bis–Tris precast, polyacrylamide gels (Invitrogen) with MES SDS running buffer (Invitrogen) in an XCell4 SureLock Midi Cell (Invitrogen) according to manufacturer's instructions. Samples were loaded for SDS-PAGE on either equal Chl (0.5 μg Chl per lane) or on equal protein (5 μg protein per lane) basis. Gels were electrophoresed at 80 V for about 3 h. For immunodetection, separated polypeptides were electroblotted onto nitrocellulose membranes (0.2 μM pore size, Bio-Rad) in transfer buffer for 1 h at 100 V. The membranes were blocked with 5 % (W/V) fat free, dried milk powder overnight at 4 °C and then probed with primary antibodies raised against the target proteins; rbcL (Hüner, University of Western Ontario, Canada), cFBPase and Lhcb1 (Agrisera AB, Vännäs, Sweden) at a dilution of 1:2,000–5,000. The blots were rinsed briefly and washed in TBS wash buffer at room temperature with agitation. The blots were probed with secondary antibody (anti-rabbit IgG peroxidase antibody, Sigma-Aldrich, Steinheim, Germany) at a 1:10,000–20,000 dilutions for 1 h at room temperature with agitation. The blots were washed as described above and the target proteins were visualized with enhanced chemiluminescence immunodetection (ECL Detection Kit; GE Healthcare, Buckinghamshire, UK) on X-ray film (Fujifilm, Fuji Corporation, Tokyo, Japan). Immunoblots were quantified by using a computer software program (SCION IMAGE, Scion Corporation, Frederick, MD, USA). For quantification, exposure times were varied to ensure that signals from the immunoblots were not saturating.

Statistical analysis

The non-acclimated WT, *BnCBF17*-OE as well as cold acclimated WT each was grown in 30 replicate pots in a completely randomized design. Out of the 30 replicate pots, three pots for each line at each growth condition were randomly selected for all measurements. Thus, all data are the means of three replicate pots. Results were subjected to analysis of variance (ANOVA). Means were compared at the 5 % level of significance ($P \leq 0.05$) by using the statistical package SPSS version 17 (IBM, Armonk, NY, USA).

Results

Growth characteristics

We carried out a pot size experiment for non-acclimated WT and *BnCBF17*-OE to ensure that pot size was large enough for proper root and sink growth at elevated CO_2 (Fig. S1). Total dry matter accumulation was significantly lower in both WT and *BnCBF17*-OE when grown in 0.3 L-sized pot (Fig. S1). However, no differences were observed in total dry matter accumulation for WT as well as *BnCBF17*-OE when grown in various pot sizes of 0.5, 1 and 1.5 L in (Fig. S1). Thus, to prevent rooting volume constraints and sink limitations, the plants were grown in 0.5 L-sized pots irrespective of growth CO_2 and growth temperatures in all experiments.

The *BnCBF17*-OE exhibited a compact, dwarf growth habit and altered leaf morphology as compared to the typical elongated growth habit for non-acclimated WT at ambient CO_2 (Fig. 1). The growth habit and plant morphology observed for *BnCBF17*-OE were comparable to those observed for cold acclimated WT at ambient CO_2

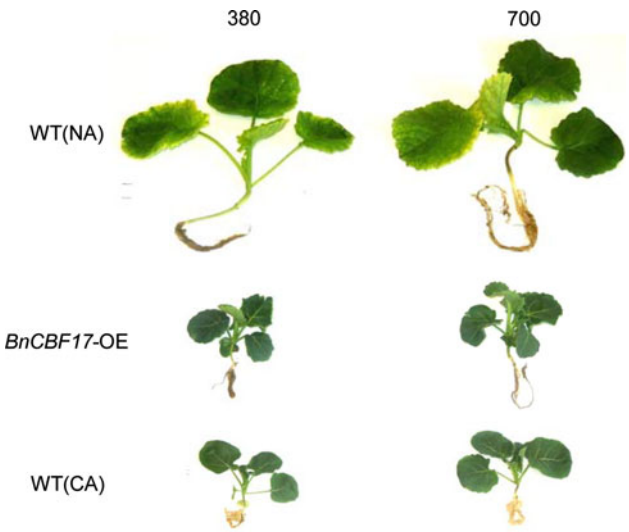

Fig. 1 Effects of cold acclimation and elevated CO_2 on plant morphology and growth habit of WT *B. napus* and *BnCBF17*-OE. The plants were grown at either ambient (380 μmol C mol^{-1}) or elevated (700 μmol C mol^{-1}) CO_2 and at either 20/16 °C (NA and *BnCBF17*-OE) or 5/5 °C (CA *Brassica* WT)

Table 1 Effects of cold acclimation and elevated CO_2 on morphological and photosynthetic characteristics of WT and *BnCBF17*-over-expressing *B. napus* grown at either ambient (380 μmol C mol^{-1}) or elevated (700 μmol C mol^{-1}) CO_2 and at either 20/16 °C (non-acclimated) or 5/5 °C (cold acclimated)

Morphological and photosynthetic characteristics	Wild type (NA)		*BnCBF17*-OE		Wild type (CA)	
	380	700	380	700	380	700
Total dry mass (mg $plant^{-1}$)	103 ± 6^{a}	124 ± 9^{b}	122 ± 10^{ab}	171 ± 14^{c}	117 ± 12^{ab}	158 ± 17^{c}
Specific leaf weight (g DM m^{-2} leaf area)	27 ± 3^{a}	36 ± 2^{b}	50 ± 6^{c}	61 ± 7^{c}	63 ± 5^{cd}	69 ± 6^{d}
Leaf Chl (mg m^{-2} leaf area)	424 ± 21^{a}	491 ± 27^{b}	942 ± 63^{d}	808 ± 41^{cd}	866 ± 39^{de}	792 ± 24^{c}
Chl-a/b ratio	3.18 ± 0.21^{b}	2.47 ± 0.28^{a}	2.82 ± 0.31^{ab}	2.84 ± 0.16^{ab}	$2.\ 76 \pm 0.17^{ab}$	2.93 ± 0.23^{ab}
Total leaf protein (g m^{-2} leaf area)	3.65 ± 0.33^{b}	2.71 ± 0.24^{a}	16.30 ± 1.52^{c}	17.23 ± 0.64^{c}	17.46 ± 1.37^{c}	15.09 ± 0.93^{c}
Protein/Chl ratio	8.61 ± 0.62^{b}	5.52 ± 0.36^{a}	17.30 ± 1.22^{c}	21.32 ± 1.51^{d}	20.16 ± 2.74^{cd}	19.05 ± 1.37^{cd}
Q (CO_2/photon)	0.045 ± 0.02^{a}	0.067 ± 0.04^{c}	0.054 ± 0.03^{b}	0.059 ± 0.03^{bc}	0.057 ± 0.05^{b}	0.063 ± 0.04^{bc}
CE (CO_2/mol^{-1} CO_2)	0.081 ± 0.03^{a}	0.073 ± 0.05^{a}	0.109 ± 0.05^{c}	0.119 ± 0.06^{c}	0.102 ± 0.08^{bc}	0.093 ± 0.06^{b}
J_{max} (μmol e^{-} m^{-2} s^{-1})	127 ± 7^{b}	101 ± 5^{a}	153 ± 8^{c}	148 ± 5^{c}	146 ± 6^{c}	152 ± 9^{c}
V_{cmax} (μmol m^{-2} s^{-1})	51 ± 4^{b}	39 ± 3^{a}	68 ± 7^{cd}	74 ± 9^{d}	63 ± 3^{cd}	60 ± 4^{bc}
R_{dark} (μmol C evolved g DW^{-1})	-0.081 ± 0.005^{c}	-0.078 ± 0.009^{c}	-0.053 ± 0.004^{ab}	-0.052 ± 0.002^{ab}	-0.048 ± 0.003^{a}	-0.059 ± 0.005^{b}

All measurements were carried out on fully developed third leaves at their respective growth CO_2 at 20 °C

Data represent the mean of three plants from three different pots ± SD

Significant differences of the means are indicated by the *superscripted letters* ($P \leq 0.05$)

(Fig. 1). Although the *BnCBF17*-OE as well as cold acclimated WT *B. napus* were smaller plants, they exhibited comparable total dry matter accumulation as that of non-acclimated WT at fully expanded third leaf stage at ambient CO_2 (Table 1). Growth at elevated CO_2 significantly increased dry matter accumulation by 20, 40 and 35 % for non-acclimated WT, *BnCBF17*-OE and cold acclimated WT, respectively relative to at ambient CO_2 (Table 1). Thus, *BnCBF17*-over-expression as well as cold acclimation appeared to substantially increase the dry matter accumulation relative to that of non-acclimated WT at elevated CO_2. The specific leaf weight (SLW) increased by about 85 % in *BnCBF17*-OE versus non-acclimated WT and by about 130 % in cold acclimated WT versus non-acclimated WT at ambient CO_2 (Table 1). Elevated CO_2 significantly stimulated SLW by 33 % in non-acclimated WT but had minimal effects in the *BnCBF17*-OE as well as in cold acclimated WT (Table 1). Consequently, at elevated CO_2, the *BnCBF17*-OE and cold acclimated WT exhibited about 70 and 90 % higher SLW, respectively compared to non-acclimated WT (Table 1).

Over-expression of *BnCBF17* substantially increased Chl per unit leaf area by about 125 % as compared to non-acclimated WT at ambient CO_2 (Table 1). The increase in Chl in the *BnCBF17*-OE was at par with the cold acclimation-induced increase in Chl per unit leaf area (105 %) for WT at ambient CO_2 (Table 1). Although, elevated CO_2 significantly increased Chl per unit leaf area by 16 % for non-acclimated WT, it significantly decreased the Chl per unit leaf area for *BnCBF17*-OE as well as cold acclimated WT by 10–15 % (Table 1). The Chl-a/b ratios decreased by about 20 % in non-acclimated WT but changed minimally in *BnCBF17*-OE and cold acclimated WT in response to growth at elevated CO_2 (Table 1).

The *BnCBF17*-OE as well as cold acclimated WT *B. napus* exhibited about 4.8-fold higher leaf protein content per unit leaf area relative to non-acclimated WT at ambient CO_2 (Table 1). Although elevated CO_2 had minimal effects on leaf protein content of the *BnCBF17*-OE as well as cold acclimated WT, elevated CO_2 appeared to significantly decrease leaf protein content by about 25 % in non-acclimated WT relative to at ambient CO_2 (Table 1). The leaf protein to Chl ratio was about twofold higher in the *BnCBF17*-OE and cold acclimated WT *B. napus* relative to non-acclimated WT at ambient CO_2 (Table 1). Elevated CO_2 reduced this ratio by about 35 % in non-acclimated WT but had minimal effects on this ratio in the *BnCBF17*-OE and cold acclimated WT *B. napus* relative to at ambient CO_2 (Table 1).

Light response curves for CO_2 assimilation

Consistent with our previous report (Dahal et al. 2012a), over-expression of *BnCBF17* (Table 1; Fig. 2b) mimicked cold acclimated WT *Brassica* (Fig. 2c) with respect to the 25 and 40 % increases in the in the apparent maximum quantum efficiency for CO_2 assimilation (Q) and the light-saturated rates of gross CO_2 assimilation (gross A_{sat}), respectively as compared to WT *B. napus* when grown and measured at ambient CO_2 (Table 1; Fig. 2a).

The sensitivity to feedback-limited rates of photosynthesis during growth at elevated CO_2 condition can be assessed by comparing CO_2 assimilation rates in plants grown under elevated (700 µmol C mol^{-1}) versus ambient CO_2 conditions (380 µmol C mol^{-1}) but measured at the same CO_2 concentration of either 380 or 700 µmol C mol^{-1}. Such a comparison revealed a significant inhibition of light- saturated rates of gross CO_2 assimilation in elevated versus ambient CO_2-grown non-acclimated WT (Fig. 2a, d) but not in either the *BnCBF17*-OE (Fig. 2b, e) or cold acclimated WT (Fig. 2c, f). Compared to growth and development at ambient CO_2, the growth and development of non-acclimated WT *B. napus* at elevated CO_2 significantly inhibited the light-saturated rates of gross CO_2 assimilation by 27 % when measured at an equal CO_2 concentration of 700 µmol C mol^{-1} (Fig. 2d). A similar inhibition of gross CO_2 assimilation (30 %) was observed between elevated versus ambient CO_2-grown non-acclimated WT when measured at an equal CO_2 concentration of 380 µmol C mol^{-1} (Fig. 2a). In contrast, light saturated rates of gross CO_2 assimilation for the *BnCBF17*-OE (Fig. 2b, e) as well as cold acclimated WT *B napus* (Fig. 2c, f) exhibited minimal sensitivity to the elevated CO_2 concentration during long-term growth and development.

CO_2-response curves for CO_2 assimilation

Figure 3 illustrates the effects of cold acclimation and elevated CO_2 on the light-saturated CO_2 response curves of net CO_2 assimilation. *BnCBF17*-over-expression (Table 1; Fig. 3b) mimicked cold acclimation of WT *Brassica* (Table 1; Fig. 3c) with respect to a 26 to 37 % increase in the carboxylation efficiency (CE) and a 35 % increase in the light and CO_2-saturated photosynthetic rates as well as

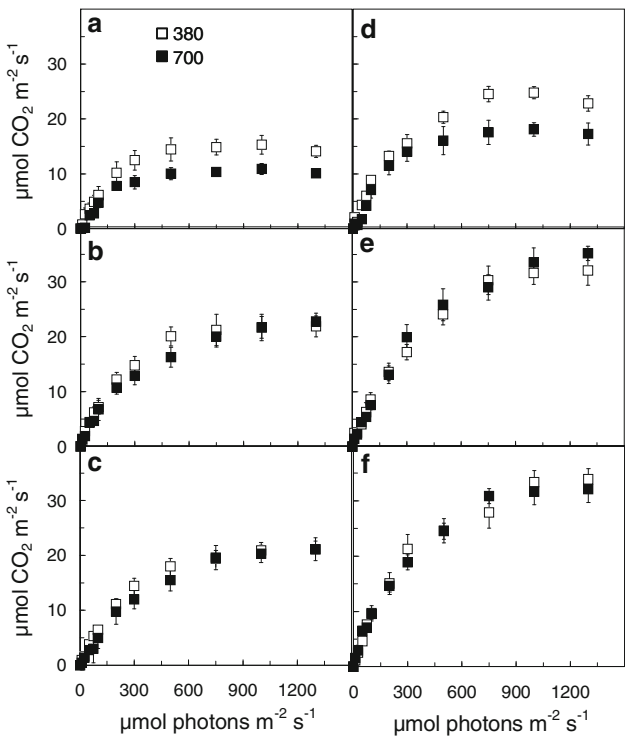

Fig. 2 Light response curves of gross CO_2 assimilation for WT (NA) (**a**, **d**), the *BnCBF17*-OE (**b**, **e**) and WT (CA) (**c**, **f**) grown at either ambient (380 µmol C mol^{-1}, *square*) or elevated (700 µmol C mol^{-1}, *filled square*) CO_2. All measurements were carried out on fully developed third leaves at 20 °C at either 380 (**a**–**c**) or 700 (**d**–**f**) µmol C mol^{-1}. Data represent the mean of three plants from three different pots. *Bars* represent SD

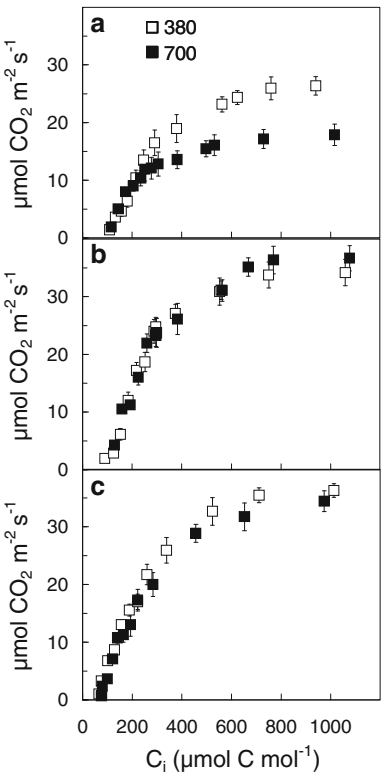

Fig. 3 CO_2 response curves of light-saturated net CO_2 assimilation for WT (NA) (**a**), the *BnCBF17*-OE (**b**) and WT (CA) (**c**) grown at either ambient (380 µmol C mol^{-1}, *square*) or elevated (700 µmol C mol^{-1}, *filled square*) CO_2. All measurements were carried out on fully developed third leaves at measuring temperature of 20 °C at a saturating irradiance of 1,300 µmol m^{-2} s^{-1} PPFD. *Data* represent the mean of three plants from three different pots. *Bars* represent SD

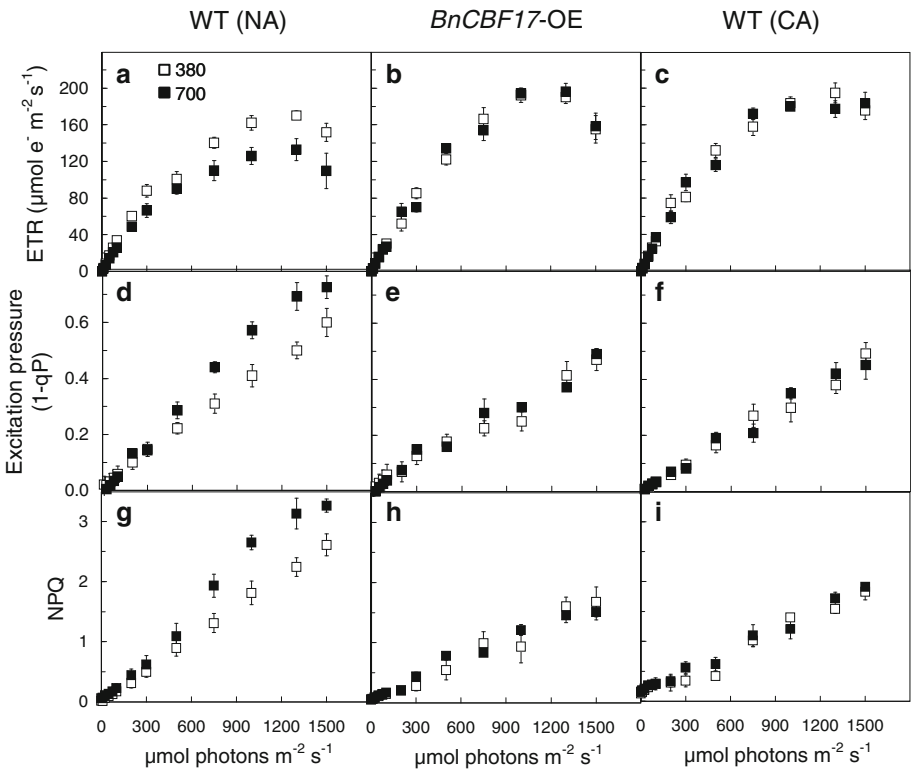

Fig. 4 Light response curves of electron transport rates (ETR; **a–c**), excitation pressures (1-qP; **d–f**) and non photochemical quenching of excess energy (NPQ; **g–i**) for non-acclimated WT (**a**, **d**, **g**), *BnCBF17*-OE (**b**, **e**, **h**) and cold acclimated WT (**c**, **f**, **i**) *B. napus* grown at either ambient (380 µmol C mol^{-1}, *square*) or elevated (700 µmol C mol^{-1}, *filled square*) CO_2 and at either 20/16 °C (NA) or 5/5 °C (CA). All measurements were carried out on fully developed third leaves at 700 µmol C mol^{-1} and at measuring temperature of 20 °C. *Data* represent the mean of three plants from three different pots. *Bars* represent SD

V_{cmax}, respectively compared to non-acclimated WT grown at ambient CO_2 (Table 1; Fig. 3a). These results are consistent with our previous reports (Dahal et al. 2012a). No significant differences in the carboxylation efficiency were observed between elevated versus ambient CO_2-grown plants for all *Brassica* lines tested (Table 1; Fig. 3). Elevated CO_2, however, significantly reduced the light and CO_2-saturated rates of net CO_2 assimilation and V_{cmax} by 32 % for non-acclimated WT (Table 1; Fig. 3a) but had minimal effects on these rates for *BnCBF17*-OE as well as cold acclimated WT (Table 1; Fig. 3b, c). The decrease in light and CO_2-saturated rates of net CO_2 assimilation observed for elevated versus ambient CO_2-grown non-acclimated WT was consistent with the decreased rates of light and CO_2-saturated electron transport in response to growth at elevated CO_2 (Table 1, J_{max}; Fig. 4a, ETR).

Light response curves for ETR, EP and NPQ

Light response curves for electron transport rates (ETR), excitation pressure (EP), measured as 1-qP and non-photochemical quenching (NPQ) (Fig. 4) were generated to estimate the apparent quantum requirement for ETR, the apparent quantum requirement to close PSII reaction centers by EP and the apparent quantum requirement to induce energy dissipation by NPQ, respectively (Dahal et al. 2012a). Apparent quantum requirement is the inverse of apparent quantum efficiency and is estimated as the inverse of the initial slopes calculated from the linear portion of the light response curve for either ETR (Fig. 4a–c), 1-qP (Fig. 4d–f) or NPQ (Fig. 4g–i).

In vivo Chl-a fluorescence indicated that *BnCBF17*-OE (Fig. 4b, open symbols) mimicked cold acclimated *Brassica* (Fig. 4c, open symbols) and exhibited a small (15 %) but significant increase in the light-saturated ETR but no change in the apparent quantum requirement for ETR (3.6–3.9 photons/e) compared to non-acclimated WT at ambient CO_2 (Fig. 4a). The data for light saturated rates of ETR measured by room temperature Chl-a fluorescence were consistent with the J_{max} based on CO_2 gas exchange (Table 1). However, the apparent quantum requirements for closure of PSII reaction centers (1,414 photons to close 50 % of PSII reaction centers) and the induction of NPQ (883 photons/unit NPQ) under ambient CO_2 conditions were 30 to 50 % greater for the *BnCBF17*-OE (Fig. 4e, h, open symbols) and cold acclimated WT *Brassica* (Fig. 4f, i, open symbols) compared with non-acclimated WT (Fig. 4d, g, open symbols).

Elevated CO_2 increased the apparent quantum requirement for ETR by 18 % and significantly inhibited the light-saturated ETR by 22 % in non-acclimated WT relative to at ambient CO_2 (Fig. 4a). The data for ETR were consistent with the J_{max} based on CO_2 gas exchange (Table 1). However, the apparent quantum requirements for PSII closure decreased significantly by about 25 % in elevated (826 photons to close 50 % PSII reaction centers) versus

ambient CO_2-grown, non-acclimated WT (1,093 photons to close 50 % PSII reaction centers) (Fig. 4d). Concomitantly, the quantum requirement to induce one unit of NPQ decreased by 30 % from 573 photons/unit NPQ to 414 photons/unit NPQ in WT grown at elevated CO_2 compared at ambient CO_2 (Fig. 4g). The decreased light and CO_2-saturated ETR for non-acclimated WT grown at elevated CO_2 was consistent with the decreased light and CO_2-saturated rates of CO_2 assimilation at elevated CO_2 (Fig. 3a). In contrast, the light response curves of ETR, EP and NPQ for the *BnCBF17*-OE as well as cold acclimated WT were insensitive to growth at elevated CO_2 (Fig. 4). This was consistent with the minimal changes in the CO_2 response curves for the *BnCBF17*-over-expressing line as well as cold acclimated WT grown under elevated versus ambient CO_2 conditions (Fig. 3b, c).

CO_2 response curves for ETR, EP and NPQ

Carbon dioxide response curves for ETR, EP and NPQ (Fig. 5) were carried out to estimate the efficiency for ETR as a function of C_i, the efficiency with which PSII reaction centers were opened by increased C_i and the efficiency with which NPQ was suppressed by increased C_i, respectively. The efficiency for ETR, EP and NPQ was estimated as the initial linear slopes of the C_i response curve for either ETR (Fig. 5a–c), 1-qP (Fig. 5d–f) or NPQ (Fig. 5g–i).

The data for the effects of C_i on ETR for plants grown under ambient CO_2 (Fig. 5a–c, open symbols) indicate that, under light-saturated conditions, the CO_2 saturated rates of ETR were 1.2-fold higher for *BnCBF17*-OE as well as cold acclimated WT than for NA WT *Brassica*. Furthermore, the efficiency of ETR in either *BnCBF17*-OE or cold acclimated WT (0.81 μmol e^- m^{-2} s^{-1}/μmol CO_2 mol^{-1}) was 1.4-fold higher than that of NA *Brassica* (0.57 μmol e^- m^{-2} s^{-1}/μmol CO_2). Growth at elevated CO_2 decreased the CO_2 saturated rates of ETR by about 33 % and the efficiency of ETR (μmol e^- m^{-2} s^{-1}/μmol CO_2 mol^{-1}) by 54 % in NA *Brassica* (Fig. 5a). In contrast, the CO_2 saturated rates of ETR as well as the efficiency of ETR were insensitive to growth of either *BnCBF17*-OE (Fig. 5b) or CA *Brassica* (Fig. 5c) at elevated CO_2. These trends were consistent with the data for the differential effects of elevated CO_2 on J_{max} in *BnCBF17*-OE and cold acclimated WT relative to non-acclimated WT *Brassica* (Table 1).

Consistent with the fact that CO_2 dominates as an ultimate electron acceptor for photosynthetic carbon assimilation, increasing C_i decreased excitation pressure in all plants tested (Fig. 5d–f) whether grown under ambient (open symbols) or elevated CO_2 (closed symbols). However, under light saturated conditions, excitation pressure at CO_2 saturation was 1.4- to 1.6-fold lower in *BnCBF17*-OE (Fig. 5e) and cold acclimated WT (Fig. 5f) than NA controls (Fig. 5d) grown at ambient CO_2 (open symbols).

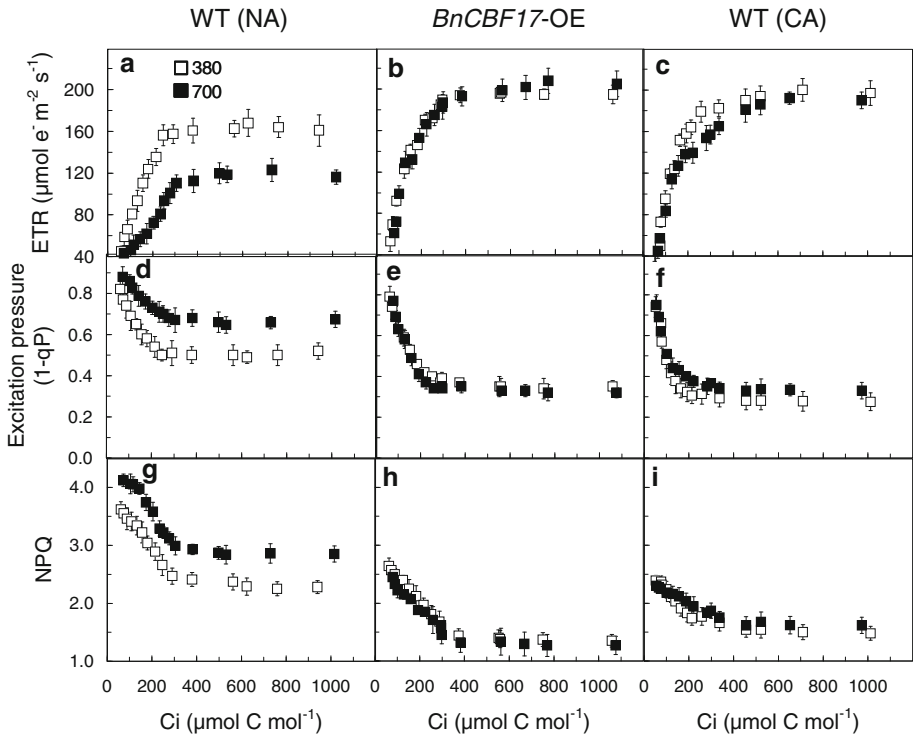

Fig. 5 CO_2 response curves of light-saturated electron transport rates (ETR; **a**–**c**), excitation pressures (1-qP; **d**–**f**) and non photochemical quenching of excess energy (NPQ; **g**–**i**) for non-acclimated WT (**a**, **d**, **g**), *BnCBF17*-OE (**b**, **e**, **h**) and cold acclimated WT (**c**, **f**, **i**) *B. napus* grown at either ambient (380 μmol C mol^{-1}, *square*) or elevated (700 μmol C mol^{-1}, *filled sqare*) CO_2 and at either 20/16 °C (NA) or 5/5 °C (CA). All measurements were carried out on fully developed third leaves at 20 °C and at a saturating irradiance of 1,300 μmol photons m^{-2} s^{-1}. Data represent the mean of three plants from three different pots. *Bars* represent SD

In addition, the efficiency with which PSII reaction centers were opened by increased CO_2 was 1.7- to 1.9-fold greater in *BnCBF17*-OE and cold acclimated WT than in non-acclimated WT (Fig. 5d–f).

Growth at elevated CO_2 not only increased the CO_2-saturated excitation pressure by about 1.4-fold in non-acclimated WT from a 1-qP of 0.48 upon growth at ambient CO_2 (open symbols) to 0.68 upon growth at elevated CO_2 (Fig. 5d, closed symbols) but also inhibited the efficiency with which PSII reaction centers were opened as a function of increased C_i by about 1.6-fold relative to non-acclimated WT *Brassica* grown at ambient CO_2 (Fig. 5d). In contrast, neither the CO_2 saturated excitation pressure nor the efficiency with PSII reaction centers were opened by increased C_i were significantly affected by growth at elevated CO_2 in *BnCBF17*-OE (Fig. 5e) as well as cold acclimated WT *Brassica* (Fig. 5f).

To complement the CO_2 response curves for excitation pressure, we also assessed the effects of changes in C_i on NPQ (Fig. 5g–i). Consistent with the fact that CO_2 is a substrate for the Rubisco-catalyzed carboxylation reaction of the Calvin cycle, increasing C_i resulted in the suppression of NPQ in non-acclimated WT (Fig. 5g), *BnCBF17*-OE (Fig. 5h) and cold-acclimated WT *Brassica* (Fig. 5i) irrespective of whether plants were grown at ambient (open symbols) or at elevated CO_2 (closed symbols). However, even at low C_i, NPQ was about 50 % lower in *BnCBF17*-OE and cold acclimated WT *Brassica* compared to non-acclimated WT. Although the response of NPQ to increasing C_i was similar whether *BnCBF17*-OE and cold acclimated WT were grown at ambient or elevated CO_2 (Fig. 5h, i, respectively), increasing C_i induced 26 % higher levels of NPQ in non-acclimated WT grown at elevated CO_2 relative to non-acclimated WT grown at ambient CO_2 (Fig. 5g).

Photosynthetic polypeptide abundance

The data in Table 1 indicate that either over-expression of *BnCBF17* or cold acclimation of WT *B. napus* resulted in a doubling of the protein/Chl ratio. When SDS-PAGE gels were loaded for immunoblot analyses on equal Chl basis (Fig. 6a), *BnCBF17* as well as cold acclimated WT *B. napus* exhibited about twofold increase in the relative amount of major stromal photosynthetic enzyme (Rubisco, rbcL) and cytosolic FBPase (cFBPase) compared to non-acclimated WT *Brassica* grown at ambient CO_2 (Fig. 6a). However, the relative amount of Lhcb1, the major protein of PSII light harvesting complex, changed minimally in *BnCBF17*-OE as well as cold acclimated WT compared to non-acclimated WT at ambient CO_2 (Fig. 6a). However, when gels were loaded on equal protein basis, the relative levels of rbcL, cFBPase and Lhcb1 changed minimally in *BnCBF17* as well as cold acclimated WT relative to non-acclimated WT at ambient CO_2 (Fig. 6b). Thus, the data in Fig. 6a and b are consistent with the increased protein/Chl ratio presented in Table 1.

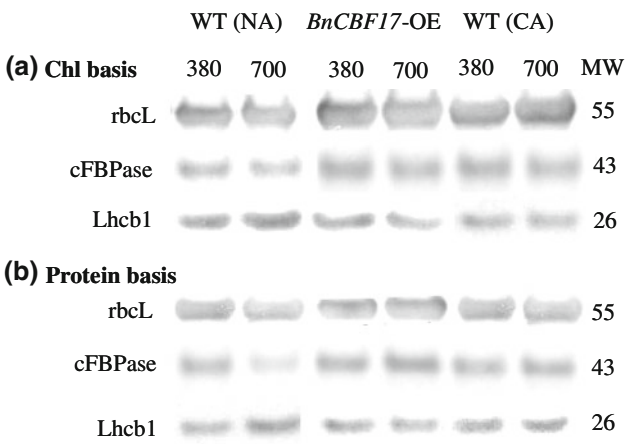

Fig. 6 Immunoblot analysis of SDS-PAGE probed with antibodies raised against: rbcL, cFBPase and Lhcb1, isolated from cold acclimated (CA) and non-acclimated (NA) wild type (WT) and *BnCBF17*-OE grown at either ambient (380 µmol C mol^{-1}) or elevated (700 µmol C mol^{-1}) CO_2 and at either 20/16 °C (NA) or 5/5 °C (CA). *Lanes* of SDS-PAGE were loaded on either equal Chl (**a**, 0.5 µg/lane) or on equal protein basis (5 µg protein/lane). The bovine serum albumin (1 µg/lane) was used as an internal control. *Numbers* on the *right* indicate molecular weight (MW, kDa) of markers

Regardless of the basis upon which the SDS-PAGE gels were loaded, growth under elevated CO_2 decreased the relative levels of rbcL by about 35 % and cFBPase by 40–70 % yet increased the relative levels of Lhcb1 by about 20 % in non-acclimated WT relative to at ambient CO_2 (Fig. 6). In contrast, growth at elevated CO_2 appeared to have minimal effects on the abundance of rbcL, cFBPase and Lhcb1 in the *BnCBF17*-OE as well as cold acclimated WT relative to at ambient CO_2 irrespective of loading basis (Fig. 6).

Stomatal characteristics

The results summarized in Table 2 are consistent with previous reports which indicate that overexpression of *BnCBF17* and cold acclimation of *B. napus* resulted in a 30 and 80 % increase in instantaneous leaf level water use efficiency (WUE) compared to non-acclimated WT grown at ambient CO_2 (Dahal et al. 2012a). This differential increase in instantaneous leaf level WUE was accounted for, in part, by differential changes in stomatal frequency (Table 2).

Elevated CO_2 suppressed leaf stomatal conductance by 20–35 % in non-acclimated, cold acclimated and the *BnCBF17*-over-expressing line of *B. napus* and, as a consequence, leaf transpiration rates decreased by 15–25 % and instantaneous leaf level WUE increased by 80–115 %

Table 2 Effects of cold acclimation and elevated CO_2 on stomatal characteristics of WT and *BnCBF17*-over-expressing *B. napus* grown at either ambient (380 μmol C mol^{-1}) or elevated (700 μmol C mol^{-1}) CO_2 and at either 20/16 °C (non-acclimated) or 5/5 °C (cold acclimated)

Stomatal characteristics	Wild type (NA)		*BnCBF17*-OE		Wild type (CA)	
	380	700	380	700	380	700
Stomatal conductance g_s (mol m^{-2} s^{-1})	0.33 ± 0.02^{c}	0.21 ± 0.03^{ab}	0.37 ± 0.03^{c}	0.30 ± 0.04^{c}	0.26 ± 0.02^{b}	0.17 ± 0.04^{a}
Stomatal frequency (stomates mm^{-2} LA)						
Adaxial	77 ± 6^{b}	47 ± 8^{a}	175 ± 23^{c}	45 ± 6^{a}	67 ± 9^{b}	48 ± 7^{a}
Abaxial	153 ± 12^{b}	84 ± 11^{a}	240 ± 34^{d}	76 ± 7^{a}	125 ± 2^{c}	63 ± 14^{a}
Transpiration (mmol H_2O m^{-2} s^{-1})	2.16 ± 0.10^{c}	1.68 ± 0.14^{ab}	2.29 ± 0.11^{c}	1.87 ± 0.16^{b}	1.74 ± 0.19^{ab}	1.52 ± 0.12^{a}
Instantaneous leaf level water use efficiency (WUE, A/g_s)	48 ± 6^{a}	104 ± 8^{c}	63 ± 4^{b}	114 ± 16^{c}	87 ± 13^{c}	168 ± 31^{d}

All measurements were carried out on fully developed third leaves at their respective growth CO_2 at 20 °C

Data represent the mean of three plants from three different pots ± SD

Significant differences of the means are indicated by the *superscripted letters* ($P \leq 0.05$)

(Table 2). It appears that the increased WUE induced by either cold acclimation or elevated CO_2 is primarily associated with an increase in light-saturated rates of CO_2 assimilation and a decrease in stomatal conductance in response to growth at either low temperature or under elevated CO_2.

The data in Table 2 indicate that the cold acclimation or elevated CO_2-induced suppression of stomatal conductance can be accounted for, in part, by a decrease in stomatal density on both the abaxial and adaxial leaf surfaces in response to growth at either low temperature or under elevated CO_2. For instance, cold acclimated WT exhibited about a 20 % decrease in adaxial as well as abaxial stomatal densities as compared to non-acclimated WT. Similarly, elevated CO_2 decreased adaxial as well as abaxial stomatal densities by 30–75 % relative to those of at ambient CO_2 for all *Brassica* plants tested (Table 2).

Dark respiratory rates

The *BnCBF17*-over-expressing line of *B. napus* exhibited a 35 % decrease in the dark respiratory rates (R_{dark}) as compared to non-acclimated WT at ambient CO_2 when expressed on per unit dry weight basis (Table 1). Dark respiratory rate observed for the *BnCBF17*-OE was comparable to that of cold acclimated WT at ambient CO_2 (Table 1). Although elevated CO_2 increased R_{dark} by about 20 % in cold acclimated WT, elevated CO_2 had minimal effects on R_{dark} of non-acclimated WT as well as *BnCBF17*-OE relative to at ambient CO_2 (Table 1).

Discussion

Compared to non-acclimated WT, *BnCBF17*-OE grown at 20 °C mimicked cold acclimated WT *B. napus* with respect to compact dwarf phenotype (Fig. 1), increased SLW (Table 1), increased photosynthetic capacity (Fig. 2), increased ETR as a function of irradiance (Fig. 4) and C_i (Fig. 5), improved instantaneous leaf level WUE (Table 1) and enhanced levels of key photosynthetic enzymes and components of photosynthetic electron transport (Fig. 6). These results are consistent with an increased quantum requirement to close PSII reaction centers and to induce energy dissipation by NPQ (Fig. 4) coupled with a lower C_i requirement to open PSII reaction centers and a lower propensity to dissipate absorbed energy through NPQ under CO_2 saturated conditions (Fig. 5). Consequently, *BnCBF17*-OE and cold acclimated WT *B. napus* exhibited a lower excitation pressure for a given irradiance and a given CO_2 concentration, and thus, a greater capacity to keep Q_A oxidized compared with non-acclimated WT *B. napus*. This indicates that compared to non-acclimated WT, *BnCBF17*-OE as well as cold acclimated WT *B. napus* exhibit an enhanced capacity to utilize absorbed light energy and convert it to biomass as reflected in an increase in SLW with a concomitant decreased reliance on NPQ to dissipate absorbed energy for photoprotection. Thus, we show that over-expression of *BnCBF17* as well as cold acclimation enhances photosynthetic energy conversion efficiency into biomass in *B. napus* coupled with enhanced instantaneous leaf level WUE during long-term growth at either ambient or elevated CO_2 conditions.We suggest that the enhanced photosynthetic capacity and energy conversion efficiency of *BnCBF17*-OE as well as cold acclimated WT relative to non-acclimated WT *B. napus* can be explained, in part, by the enhanced abundance, on a Chl basis, of major regulatory photosynthetic enzymes such as stromal-localized Rubisco (rbcL) and cytosolic FBPase (cFBPase) important in regulating sucrose biosynthesis as well as components of the thylakoid membrane represented by Lhcb1 (Fig. 6a). We suggest that

the increased protein/Chl ratio (Table 1) reflects an increase in components of the thylakoid photosynthetic electron transport chain, Calvin cycle enzymes involved in the assimilation of CO_2 as well as cytosolic sucrose biosynthetic enzymes on a leaf area basis. These results for the *BnCBF17*-OE and cold acclimated *B. napus* are comparable to the enhanced photosynthetic performance reported recently for cold acclimated winter wheat and winter rye (Dahal et al. 2012a). In the cold acclimated winter cereals, the enhanced photosynthetic performance was shown to be due to increased levels of photosynthetic proteins (e.g., rbcL, psbA, psaA, cFBPase, Lhcb1) per leaf area combined with a decrease in the low temperature sensitivity of ETR and CO_2 assimilation (Dahal et al. 2012a). *BnCBF17*-OE also exhibited a similar low temperature insensitivity for ETR and CO_2 assimilation as did the cold acclimated winter cereals (Dahal et al. 2012a). This is consistent with the report of Savitch et al. (2005) who reported that the *BnCBF17*-OE exhibited significant enhancement for the gene expression as well as enzyme activities of Rubisco, SPS and cFBPase. Therefore, we suggest that the enhanced photosynthetic performance and energy conversion efficiency of *BnCBF17*-OE and cold acclimated WT *B. napus* is due to increased amount of photosynthetic apparatus per unit leaf area combined with a decrease in the low temperature sensitivity of ETR and CO_2 assimilation. Despite the 40–50 % lower leaf area for light interception for both *BnCBF17*-OE and the cold acclimated WT relative to non-acclimated WT, the former exhibited a 14–18 % increase in total dry weight (Table 1). Thus, the enhanced SLW observed for *BnCBF17*-OE and the cold acclimated WT compensates for the decrease in total leaf area for light absorption relative to WT non-acclimated controls. Recently, Murchie et al. (2009) discussed the challenges of increasing energy conversion efficiency in order to enhance crop biomass production and harvestable yield per hectare. We suggest that CBFs/DREBs may be critical factors that govern plant phenotypic plasticity associated not only with cold acclimation from the level of gene expression and freezing tolerance but also whole plant architecture, instantaneous leaf level WUE and photosynthetic energy conversion efficiency into biomass.

The photosynthetic response of C_3 plants to CO_2 has been theoretically modeled by Farquhar's group (Farquhar et al. 1980). According to their model, at higher C_i, CO_2 assimilation is usually limited either by the capacity of photosynthetic electron transport to supply ATP and NADPH to regenerate RuBP, or by the capacity of starch and sucrose synthesis to utilize triose phosphates and consequently regenerate P_i. The P_i regeneration-limited photosynthesis is governed by the balance between the source leaves to assimilate carbon and the sink strength to utilize photoassimilates (Arp 1991; Drake et al. 1997). It has been suggested that the increased carbon uptake resulting from initial stimulation of photosynthesis alters the balance between supply and demand due to limited sink capacity to utilize carbohydrates and concomitant retardation of carbon export to the sinks (Kramer 1981; Arp 1991; Drake et al. 1997). This results in the accumulation of sucrose in the source leaves followed by inhibition of sucrose synthesis and a short-term decrease in utilization of phosphorylated intermediates and depletion in stromal P_i. Low availability of stromal P_i triggers inhibition of ATP synthesis and thereby a decrease in the rate at which PGA is converted to triose phosphate which results in feedback inhibition of CO_2 assimilation (Stitt and Quick 1989; Sharkey and Vanderveer 1989).

The light response curves (Fig. 2) as well as CO_2 response curves (Fig. 3) clearly indicated that the light and CO_2-saturated rates of photosynthesis were significantly lower in elevated versus ambient-CO_2 grown non-acclimated WT *B. napus*. This was consistent with the decreased CO_2-saturated rates of electron transport (Fig. 4a) combined with decreased levels of major photosynthetic enzymes such as rbcL, cFBPase (Fig. 6) as well as the maximum carboxylation velocity of Rubisco in elevated versus ambient CO_2-grown non-acclimated WT (Table 1). Consequently, the EP and NPQ at any given irradiance and CO_2 concentration increased significantly for non-acclimated WT in response to growth at elevated CO_2 (Figs. 4, 5). In contrast, *BnCBF17*-OE as well as cold acclimated WT did not exhibit inhibition of light and CO_2-saturated rates of photosynthesis in response to growth at elevated CO_2 (Figs. 2, 3). This was consistent with no changes in the light and CO_2-saturated rates of electron transport, excitation pressure and NPQ (Figs. 4, 5) and levels of rbcL and cFBPase (Fig. 6) as well as the maximum carboxylation velocity of Rubisco (Table 1) in elevated versus ambient CO_2-grown *BnCBF17*-OE and cold acclimated WT *B. napus*. Thus, we report that the cold acclimated *B. napus* and the *BnCBF17*-OE are able to maintain enhanced photosynthetic performance and energy conversion into biomass even under long-term growth and development at elevated CO_2. This appears to be due to a decreased sensitivity to feedback limited photosynthesis in *BnCBF17*-OE as well as cold acclimated *B. napus* relative to non-acclimated WT plants.

How does *BnCBF17* over-expression and cold acclimation of WT *B. napus* differentially affect sensitivity to feedback inhibition of photosynthesis at elevated CO_2? Our results indicate that the *BnCBF17*-OE as well as cold acclimated WT exhibit a 1.7–1.9-fold higher specific leaf weight relative to non-acclimated WT at elevated CO_2 (Table 1). We have further shown that *BnCBF17*-over-expression as well as cold acclimation results in the enhanced amounts of rbcL and cFBPase (Fig. 6) when corrected on a leaf area basis not only at ambient CO_2 but also at elevated CO_2. This is consistent with our previous reports that cold acclimation

of winter cereals induces an increase in the amount of Rubisco and cFBPase with a concomitant stimulation of respiration and plant biomass production (Dahal et al. 2012a). Furthermore, Savitch et al. (2005) reported that over-expression of *BnCBF17* in *B. napus* not only enhanced gene expression of the triose-P translocator and cFBPase but also increased the activity of Rubisco, cFBPase and SPS. Consequently, *BnCBF17*-over-expression as well as cold acclimation of *B. napus* result in enhanced P_i cycling and increased capacity for RuBP regeneration through increased utilization of phosphorylated intermediates. Thus, we suggest that the decreased sensitivity to feedback limited photosynthesis in cold acclimated *B. napus* as well as the *BnCBF17*-OE under conditions of elevated CO_2 reflects an improved capacity to maintain a high flux of carbon between source and sink even under elevated CO_2 conditions. This is further supported by the fact that in cereals, carbon export rates from source leaves are also enhanced upon cold acclimation (Leonardos et al. 2003).

The improved instantaneous leaf level WUE induced by either *BnCBF17*-over-expression or cold acclimation is primarily associated with an increase in A_{sat} and decrease in stomatal conductance. It appears that the suppressed stomatal conductance observed upon cold acclimation or *BnCBF17*-over-expression can be accounted for, in part, by a decrease in stomatal density on both the abaxial and adaxial leaf surfaces.

We conclude that the over-expression of *BnCBF17* and cold acclimation of *B. napus* enhances photosynthetic performance, the efficiency of energy conversion and instantaneous leaf level WUE which is maintained even after long-term growth and development under elevated CO_2 conditions. Thus, we suggest that the transcription factor, *BnCBF17*, may be a central component which governs the regulation of plant architecture, photosynthetic capacity and energy conversion efficiency of crops. This may provide important new insights into potential molecular and genetic approaches focussed on the maintenance or even the enhancement of plant productivity under sub-optimal growth conditions associated with climate change.

Acknowledgments This work was supported, in part, by the Natural Sciences and Engineering Research Council (NSERC) and industrial and government partners, through the Green Crop Research Network (GCN). NPAH also acknowledges research support through an individual NSERC Discovery Grant, the Canada Research Chair program as well as the Canada Foundation for Innovation.

References

Adams WW III, Demmig-Adams B, Rosenstiel TN, Brightwell AK, Ebbert V (2002) Photosynthesis and photoprotection in over-wintering plants. Plant Biol 4:545–557

Ainsworth EA, Rogers A (2007) The response of photosynthesis and stomatal conductance to rising CO_2: mechanisms and environmental interactions. Plan Cell Environ 30:258–270

Arnon DI (1949) Copper enzymes in isolated chloroplasts Polyphenoloxidases in Beta vulgaris. Plant Physiol 24:1–15

Arp WJ (1991) Effects of source—sink relations on photosynthetic acclimation to elevated CO_2. Plant Cell Environ 14:869–875

Badawi M, Reddy YV, Agharbaoui Z, Tominaga Y, Danyluk J, Sarhan F, Houde M (2008) Structure and functional analysis of wheat *ICE* (inducer of CBF expression) genes. Plant Cell Physiol 49:1237–1249

Boese SR, Hüner NPA (1990) Effect of growth temperature and temperature shifts on spinach leaf morphology and photosynthesis. Plant Physiol 94:1830–1836

Boese SR, Hüner NPA (1992) Developmental history affects the susceptibility of spinach leaves to in vivo low temperature photoinhibition. Plant Physiol 99:1141–1145

Cheng SH, Moore BD, Seemann JR (1998) Effects of short and long-term elevated CO_2 on the expression of Ribulose-1,5-bisphosphate carboxylase/oxygenase genes and carbohydrate accumulation in leaves of *Arabidopsis thaliana* (L.) Heynh. Plant Physiol 116:715–723

Chinnusamy V, Zhu J, Zhu JK (2007) Cold stress regulation of gene expression in plants. Trends Plant Sci 12:1360–1385

Dahal K, Kane K, Gadapati W, Webb E, Savitch LV, Singh J, Sharma P, Sarhan F, Longstaffe FJ, Grodzinski B, Hüner NPA (2012a) The effects of phenotypic plasticity on photosynthetic performance in winter rye, winter wheat and *Brassica napus*. Physiol Plant 144:169–188

Dahal K, Kane K, Sarhan F, Grodzinski B, Hüner NPA (2012b) Cold acclimation inhibits CO_2-dependent stimulation of photosynthesis in spring wheat and spring rye. Botany 90 (in press). doi: 10.1139/B2012-007

Drake BG, Gonzàlez-Meler MA, Long SP (1997) More efficient plants: a consequence of rising atmospheric CO_2? Annu Rev Plant Physiol Plant Mol Biol 48:609–639

Ensminger I, Busch F, Hüner NPA (2006) Photostasis and cold acclimation: sensing low temperature through photosynthesis. Physiol Plant 126:28–44

Farquhar GD, Caemmerer S, Berry JA (1980) A biochemical model of photosynthetic CO_2 assimilation in leaves of C_3 species. Planta 149:78–90

Foyer C (1990) The effect of sucrose and mannose on cytoplasmic protein phosphorylation sucrose phosphate synthetase activity and photosynthesis in leaf protoplasts from spinach. Plant Physiol Biochem 28:151–160

Gilmour SJ, Fowler SG, Thomashow MF (2000) Arabidopsis transcriptional activators CBF1, CBF2 and CBF3 have matching functional activities. Plant Mol Biol 54:767–781

Gilmour SJ, Sebolt AM, Salazar MP, Everard JD, Thomashow MF (2004) Over-expression of the *Arabidopsis* CBF3 transcriptional activator mimics multiple biochemical changes associated with cold acclimation. Plant Physiol 124:1854–1865

Gorsuch PA, Pandey S, Atkin OK (2010a) Thermal de-acclimation: how permanent are leaf phenotypes when cold-acclimated plants experience warming? Plant Cell Environ 33:1124–1137

Gorsuch PA, Pandey S, Atkin OK (2010b) Temporal heterogeneity of cold acclimation phenotypes in *Arabidopsis* leaves. Plant Cell Environ 33:244–258

Gray GR, Chauvin LP, Sarhan F, Huner NPA (1997) Cold acclimation and freezing tolerance. A complex interaction of light and temperature. Plant Physiol 114:467–474

Guy CL (1990) Cold acclimation and freezing tolerance: role of protein metabolism. Annu Rev Plant Physiol Plant Mol Biol 41:187–223

Harley PC, Sharkey TD (1991) An improved model of C_3 photosynthesis at high CO_2: reversed O_2 sensitivity explained by lack of glycerate reentry into the chloroplast. Photosynth Res 27:169–178

Hüner NPA (1985) Morphological, anatomical and molecular consequences of growth and development at low temperature in *Secale cereale* L. cv Puma. Amer J Bot 72:1290–1306

Hüner NPA, Palta JP, Li PH, Carter JV (1981) Anatomical changes in leaves of Puma rye in response to growth at cold hardening temperatures. Bot Gaz 142:55–62

Hüner NPA, Öquist G, Hurry VM, Krol M, Falk S, Griffith M (1993) Photosynthesis, photoinhibition and low temperature acclimation in cold tolerant plants. Photosyn Res 37:19–39

Hüner NPA, Öquist G, Sarhan F (1998) Energy balance and acclimation to light and cold. Trend Plant Sci 3:224–230

Hurry V, Strand A, Furbank R, Stitt M (2000) The role of inorganic phosphate in the development of freezing tolerance and the acclimatization of photosynthesis to low temperature is revealed by the pho mutants of *Arabidopsis thaliana*. Plant J 24:383–396

Jahnke S (2001) Atmospheric CO_2 concentration does not directly affect leaf respiration in bean or poplar. Plant Cell Environ 24:1139–1151

Jahnke S, Krewitt M (2002) Atmospheric CO_2 concentration may directly affect leaf respiration measurement in tobacco, but not respiration itself. Plant Cell Environ 25:641–651

Kasuga M, Liu Q, Miura S, Yamaguchi-Shinozaki K, Shinozaki K (1999) Improving plant drought, salt, and freezing tolerance by gene transfer of a single stress-inducible transcription factor. Nat Biotech 17:287–291

Kramer PJ (1981) Carbon dioxide concentration, photosynthesis and dry matter production. Bio Sci 31:29–33

Krause GH (1988) Photoinhibition of photosynthesis. An evaluation of damaging and protective mechanisms. Physiol Plant 74:566–574

Leonardos ED, Savitch LV, Huner NPA, Öquist G, Grodzinski B (2003) Daily photosynthetic and C-export patterns in winter wheat leaves during cold stress and acclimation. Plant Physiol 117:521–531

Liu Q, Kasuga M, Sakuma Y, Abe H, Miura S, Yamaguchi-Shinozaki K, Shinozaki K (1998) Two transcription factors, DREB1 and DREB2, with an EREBP/AP2 DNA binding domain separate two cellular signal transduction pathways in drought- and low-temperature-responsive gene expression, respectively, in *Arabidopsis*. Plant Cell 10:1391–1406

Long SP, Ainsworth EA, Rogers A, Ort DR (2004) Rising atmospheric carbon dioxide: plants FACE the future. Annu Rev Plant Biol 55:591–628

Moore BD, Cheng SH, Sims D, Seemann JR (1999) The biochemical and molecular basis for photosynthetic acclimation to elevated atmospheric CO_2. Plant Cell Environ 22:567–582

Murchie EH, Pinto M, Horton P (2009) Agriculture and the new challenges for photosynthesis research. New Phytol 181:532–552

Navarro M, Ayax C, Martinez Y, Laur J, Kayal WEI, Marque C, Teulieres C (2011) Two *EguCBF1* genes overexpressed in *Eucalyptus* display a different impact on stress tolerance and plant development. Plant Biotech J 9:50–63

Öquist G, Hüner NPA (2003) Photosynthesis of overwintering evergreen plants. Annu Rev Plant Biol 54:329–355

Öquist G, Hurry VM, Hüner NPA (1993) Low-temperature effects on photosynthesis and correlation with freezing tolerance in spring and winter cultivars of wheat and rye. Plant Physiol 101:245–250

Pino M-T, Skinner JS, Jeknic Z, Hayes PM, Soeldner AH, Thomashow MF, Chen THH (2008) Ecotopic *AtCBF1* overexpression enhances freezing tolerance and induces cold acclimation-associated physiological modifications in potato. Plant Cell Environ 31:393–406

Pocock TH, Hurry VM, Savitch LV, Hüner NPA (2001) Susceptibility to low-temperature photoinhibition and the acquisition of freezing tolerance in winter and spring wheat: the role of growth temperature and irradiance. Physiol Plant 113:499–506

Sarhan F, Ouellet F, Vazquez-Tello A (1997) The wheat *Wcs120* gene family: a useful model to understand the molecular genetics of freezing tolerance in cereals. Physiol Plant 101:439–445

Savitch LV, Barker-Astrom J, Ivanov AG, Hurry V, Oquist G, Hüner NPA (2001) Cold acclimation of *Arabidopsis thaliana* results in incomplete recovery of photosynthetic capacity which is associated with an increased reduction of the chloroplast stroma. Planta 214:295–301

Savitch LV, Allard G, Seki M, Robert LS, Tinker NA, Hüner NPA, Shinozaki K, Singh J (2005) The effect of over-expression of two *Brassica* CBF/DREB1-like transcription factors on photosynthetic capacity and freezing tolerance in *Brassica napus*. Plant Cell Physiol 46:1525–1539

Sharkey TD, Vanderveer PJ (1989) Stromal phosphate concentration is low during feedback limited photosynthesis. Plant Physiol 91:679–684

Somersalo S, Krause GH (1989) Photoinhibition at chilling temperatures: fluorescence characteristics of unhardened and cold-hardened spinach leaves. Planta 177:409–416

Stitt M, Hurry VM (2002) A plant for all seasons: alterations in photosynthetic carbon metabolism during cold acclimation in *Arabidopsis*. Curr Opin Plant Biol 5:199–206

Stitt M, Quick WP (1989) Photosynthetic carbon partitioning: its regulation and possibilities for manipulation. Physiol Plant 77:633–641

Strand A, Hurry VM, Henkes S, Hüner NPA, Gustafsson P, Gardeström P, Stitt M (1999) Acclimation of *Arabidopsis* leaves developing at low temperatures. Increasing cytoplasmic volume accompanies increased activities of enzymes in the Calvin cycle and in the sucrose-biosynthesis pathway. Plant Physiol 119:1387–1398

Tcherkez GGB, Farquhar GD, Andrews TJ (2006) Despite slow catalysis and confused substrate specificity, all ribulose bisphosphate carboxylases may be nearly perfectly optimized. Proc Nat Acad Sci 103:7246–7251

Van Buskirk HA, Thomashow MF (2006) *Arabidopsis* transcription factors regulating cold acclimation. Physiol Plant 126:72–80

Yang J-S, Wang R, Meng J–J, Bi Y-P, Xu P-L, Guo F, Wan S-B, He Q-W, Li X-G (2010) Overexpression of *Arabidopsis* CBF1 gene in transgenic tobacco alleviates photoinhibition of PSII and PSI during chilling stress under low irradiance. J Plant Physiol 167:534–539

Zhang X, Fowler SG, Cheng H, Lou Y, Rhee SY, Stockinger EJ, Thomashow MF (2004) Freezing-sensitive tomato has a functional CBF cold responsive pathway but a CBF regulon that differs from that of freezing tolerant *Arabidopsis*. Plant J 39:905–919